Two-Dimensional Adaptive-Wall Tests in the NASA Ames Two- by Two-Foot Transonic Wind Tunnel

Edward T. Schairer* and George Lee†
NASA Ames Research Center, Moffett Field, California 94035
and
T. Kevin McDevitt‡
Complere, Inc., Palo Alto, California 94302

This paper describes the first tests conducted in the adaptive-wall test section of the 2- × 2-ft transonic wind tunnel at NASA Ames Research Center. The purpose of the tests was to demonstrate an automatic procedure for minimizing two-dimensional wall interference by actively controlling flow through the slotted upper and lower walls of the test section. Flow through the walls was regulated by adjusting pressures in compartments of a segmented plenum. The procedure for determining the necessary pressure adjustments consisted of the following steps: 1) using a fast-scanning, two-component laser velocimeter to measure flow velocities along axial lines above and below the model; 2) testing the flow measurements for compatibility with free-air, far-field boundary conditions; and 3) using empirical influence coefficients to relate changes in flow velocity to changes in plenum pressures. A NACA 0012 airfoil was tested at Mach numbers between 0.70 and 0.85 and at angles of attack of 0 and 2 deg. In all cases, the procedure substantially reduced wall interference; however, measurable and significant interference persisted after the final plenum-pressure adjustments. The principal reason that interference could not be completely eliminated was that the effects of the plenum-pressure adjustments on the velocity measurements could not be predicted accurately.

Nomenclature

C_n = normal force coefficient
C_p = pressure coefficient
c = model chord length
M = freestream Mach number
p = pressure, lb/in.^{2}
p^t = total pressure, lb/in.^{2}
R = Reynolds number
U = freestream velocity
u = axial perturbation velocity
w = vertical velocity
x, ξ = axial distance from model leading edge, positive downstream
z, η = distance above test section centerline
α = angle of attack, deg
β = $\sqrt{1-M^2}$

Subscripts

m = model induced (free air)
p = in pressure manifold
v = in vacuum reservoir
w = wall induced
∞ = freestream

Introduction

SINCE the early 1970s there has been widespread interest in developing test sections with adjustable, or adaptive, walls as a means of minimizing or eliminating wall interference. Such test sections would be particularly valuable in simulating nonlinear flows (e.g., transonic flows and low-speed, high-lift flows) for which conventional methods of accounting for wall interference are inadequate. The key idea that makes adaptive-wall test sections practical, and distinguishes them from earlier test sections with adjustable walls, is that the wall settings for minimum interference can be determined from flow measurements along a contour surrounding the model, without any information about the model.[1]

Research worldwide has focused on two types of test sections: those with solid but flexible walls that are bent to conform to the shapes of free-air streamlines; and those with rigid, ventilated walls in which the flow through the walls is controlled by adjusting either the wall porosity or the pressure difference through the wall. The flexible-wall approach is attractive because the walls themselves can serve as the contour, and the wall shape and pressure distribution (both of which can be measured quickly and easily) can be used as the flow boundary conditions. In addition, the wall shape can be controlled directly and quickly. There must be some accounting, however, for the effect of the wall boundary layers on the streamline shape. This effect becomes especially unpredictable when the shock wave from the model extends to the wall. Flexible-wall technology for two-dimensional transonic testing has been well developed, and there are currently two test sections, one in NASA Langley Research Center's 0.3-m wind tunnel[2] and the other in the Office National d'Etudes et de Recherches Aérospatiales' (ONERA) T2 wind tunnel,[3] that are used for transonic testing on a production basis. Also noteworthy is the success at Southampton University in adapting a fully choked channel.[4]

The utility of using passive ventilated walls to reduce wall interference at transonic speeds has been well established over the past 40 years. Therefore, active control of flow through ventilated walls represents a refinement of a proven concept. An advantage of the ventilated-wall approach is that, with proper segmentation of the wall panels or plenum, it can be applied for three-dimensional testing. In contrast, flexible walls present difficult mechanical problems in three dimensions since the required wall shapes may include double curvature. In a ventilated-wall test section, however, the flow mea-

Received Sept. 27, 1989; revision received Sept. 21, 1990; accepted for publication Oct. 22, 1990.

*Research Scientist, Fluid Dynamics Research Branch.
†Assistant Chief, Fluid Dynamics Research Branch.
‡Research Associate.

surements must be made in the inviscid flow outside the wall boundary layer because the flow at the walls is generally very complicated. This presents not only a difficult flow-measurement problem, but also a problem in relating the measurements to the settings of the wall controls.

At NASA Ames Research Center, we chose to develop adaptive-wall test sections with slotted walls and segmented plenums for the following reasons: 1) most of the transonic wind tunnels at NASA Ames have slotted walls; 2) the slats between the slots provide space for windows; and 3) this approach seemed promising for three-dimensional testing. Two-dimensional airfoil tests were first conducted in a small test section with longitudinally slotted top and bottom walls, plexiglass sidewalls, and upper and lower plenums that were each divided into 10 compartments.[5] The flow-measurement problem was simplified by developing a linear interference assessment algorithm that requires measurements of only one component of velocity[6]; the measurements were made using a laser velocimeter. The plenum-pressure changes needed to reduce interference were determined from empirical influence coefficients. All aspects of the experiment were automated, except that the valves for controlling pressures in the plenum components were adjusted manually.

Encouraged by the success of these pilot tests, we decided to apply the same methods in the NASA Ames 2- × 2-ft transonic wind tunnel, a facility suitable for production testing. Improvements compared to the pilot test section were to include the following: 1) more plenum compartments, 2) automatic wall control, 3) the capability to measure two components of velocity rather than just one, and 4) interference assessment that would account for nonlinear effects. In addition, a new control system would be required for existing pumps to supply high- and low-pressure air to the test station.

This paper describes the results of the first tests conducted in the new test section. The purpose of the tests was to verify the operation of the test section and its systems and to demon-

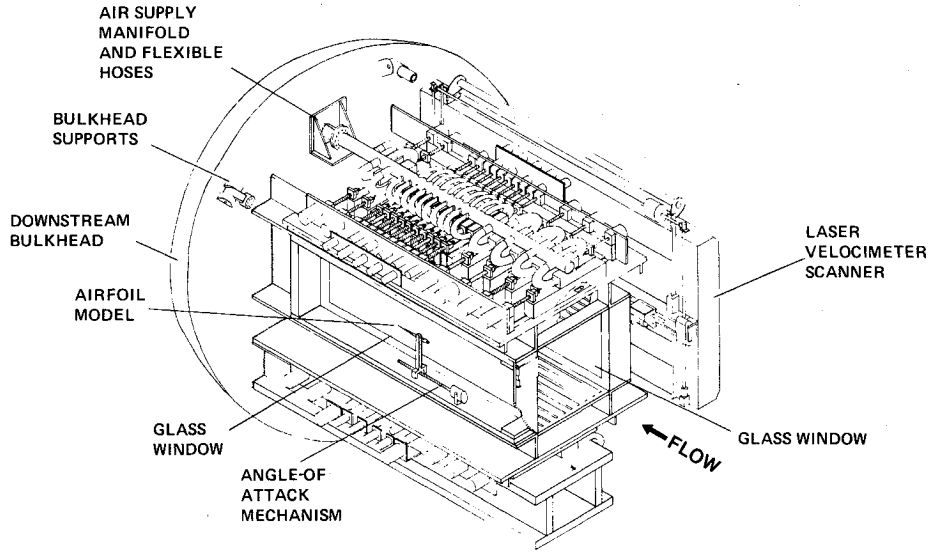

Fig. 1 2- × 2-ft adaptive-wall test section.

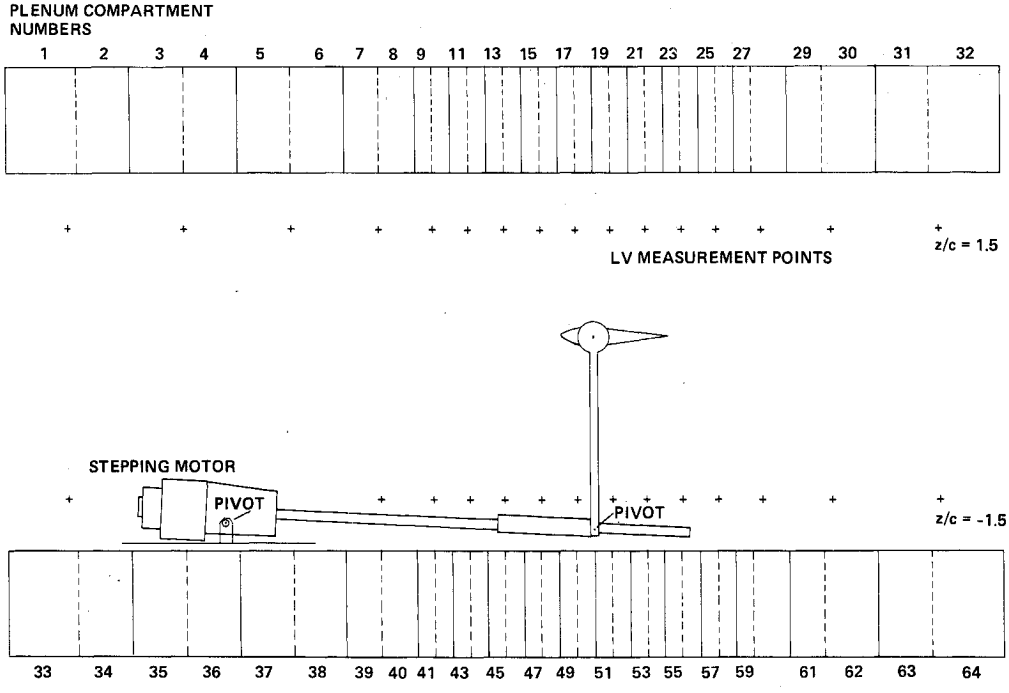

Fig. 2 Side view of the test section showing plenum compartments, LV measurement points, model, and angle-of-attack mechanism.

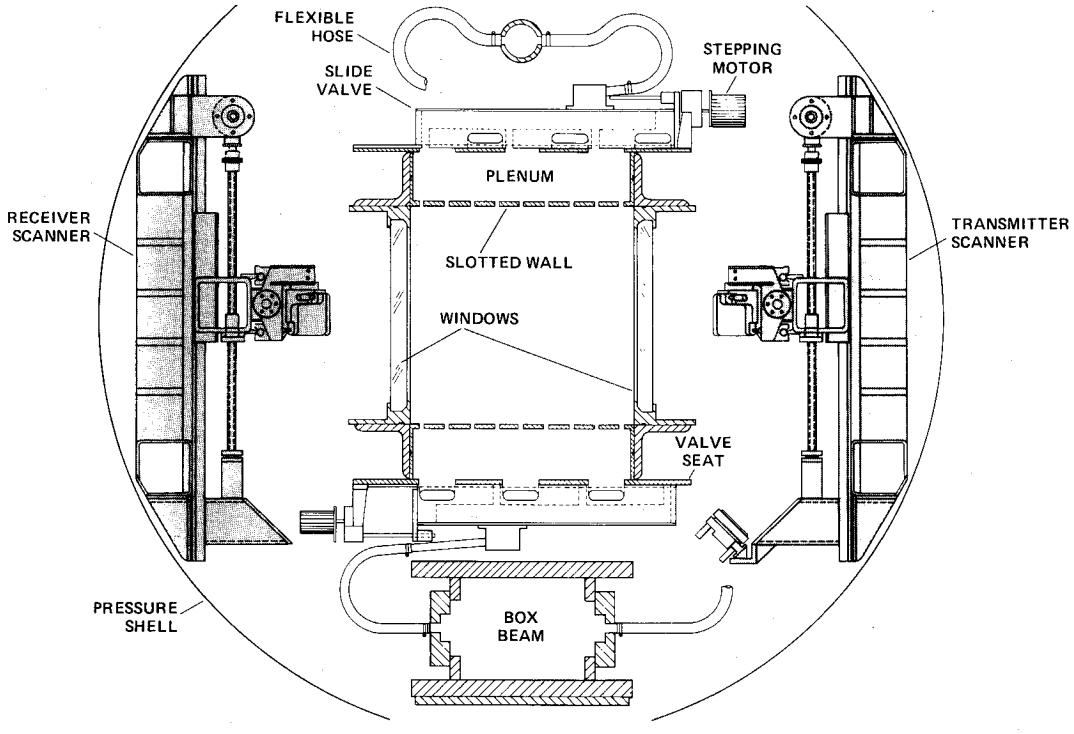

Fig. 3 Lateral cross section of the test section.

strate an automatic procedure for measuring and reducing wall interference.

Equipment

Wind Tunnel and Test Section

The 2- × 2-ft transonic wind tunnel is a closed-return tunnel capable of operating at Mach numbers up to 1.4 and pressures between 0.1 and 3.0 atm. The adaptive-wall test section (Fig. 1) was mounted between circular pressure bulkheads and inside a cylindrical pressure shell that sealed the space between the bulkheads. In Fig. 1, the upstream bulkhead and pressure shell are omitted so that the test section can be shown more clearly. The space between the bulkheads was evacuated by an auxiliary pump and served as the low-pressure-air reservoir. A structural box beam below the test section and a 4-in.-diam pipe above the test section were pressurized by a second auxiliary pump and served as the high-pressure-air reservoirs.

The test section was 2-ft high, 2-ft wide, and approximately 5-ft long. The top and bottom walls each included nine equally spaced, open longitudinal slots (open-area ratio = 0.14), and the sidewalls were solid-glass windows. Separate plenums above and below the test section were each divided into 32 compartments of varying size by spanwise partitions (Fig. 2). Pressures in the compartments were controlled by three-way, proportional slide valves that were connected to the high- and low-pressure reservoirs. Stepping motors drove the slide valves in the spanwise direction along a valve seat that formed the back of the plenum (Fig. 3). Depending on the position of the valve, ports in the valve seat were either closed or open to one of the reservoirs, allowing air to be injected into or removed from the test section. In Fig. 3, the top and bottom valves are in the positions corresponding to maximum air injection and removal, respectively.

Model and Angle-of-Attack System

The model was a 6-in.-chord NACA 0012 airfoil. A ¾-in.-diam shaft extended from each end of the model at 30% chord and protruded through holes in the sidewall windows. Lift and drag loads were transferred from the model to the glass through spherical bearings. Pitching and bending moments were transferred to the window frames by the angle-of-attack-setting mechanisms on either side of the test section (Fig. 2). Each mechanism was driven by a stepping motor fitted with a mechanical encoder and a fail-safe brake. All tests were conducted without a boundary-layer trip, and the position of transition to turbulence was unknown. Model surface pressures were measured at orifices along the midspan.

Instrumentation

Laser Velocimeter

The laser velocimeter (LV) was a two-component, on-axis, forward-scatter system in which the light source was a 5-W argon-ion laser. It was designed to measure axial and vertical velocities at virtually any point in the plane midway between the test-section sidewalls and to move rapidly between measurement points. The system is illustrated schematically in Fig. 4.

The laser and optics for generating four parallel laser beams were mounted on a stationary optics table in the control room. The vertical-velocity channel was Bragg-shifted by 40 MHz to avoid directional ambiguity. The transmitting and collecting lenses were mounted on separate two-dimensional positioning mechanisms (scanners) that were mounted on opposite sides of the test section and within the pressure shell (Fig. 3). The laser beams from the optics table were directed through a window in the pressure shell and then to the transmitting lens by a series of turning mirrors on the transmitter scanner.

The velocimeter was unusual inasmuch as the transmitting and collecting lenses were positioned along the same optical axis and a retroreflector was mounted behind the collecting lens. This arrangement allowed forward-scattered light to be returned to the transmitting lens much as if it had been directly back-scattered. The design exploited the much higher signal strength of a forward-scatter system compared to a back-scatter system and was much less sensitive to misalignment between the transmitting and collecting lenses than a conventional, off-axis, forward-scatter system. As in a conventional back-scatter system, the photomultiplier tubes and the optics for color separating the collected light were mounted on the optics table.

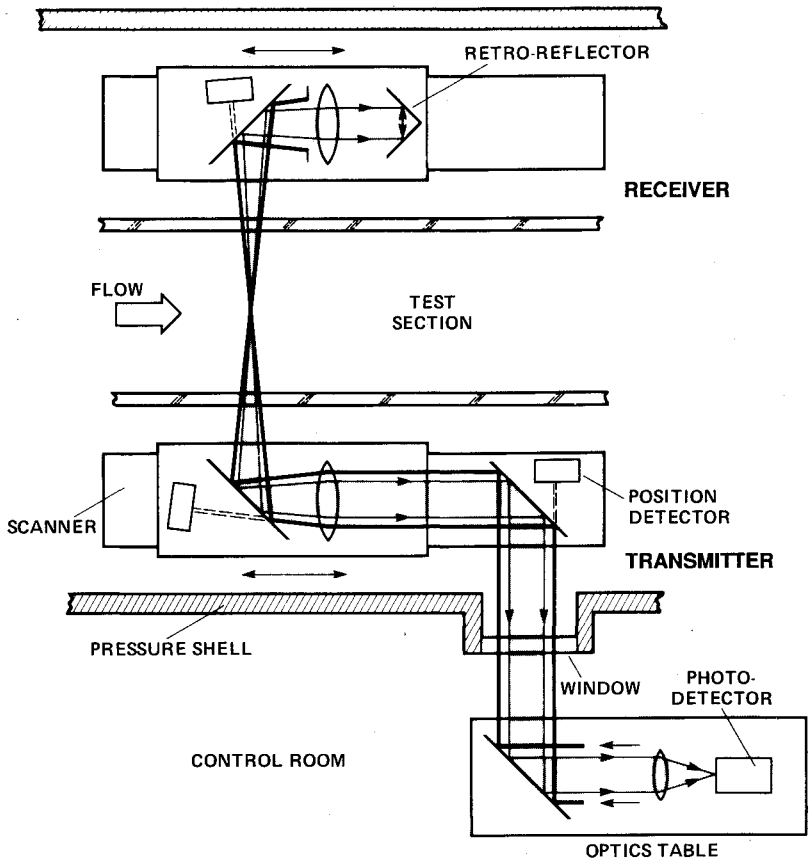

Fig. 4 Schematic of laser velocimeter.

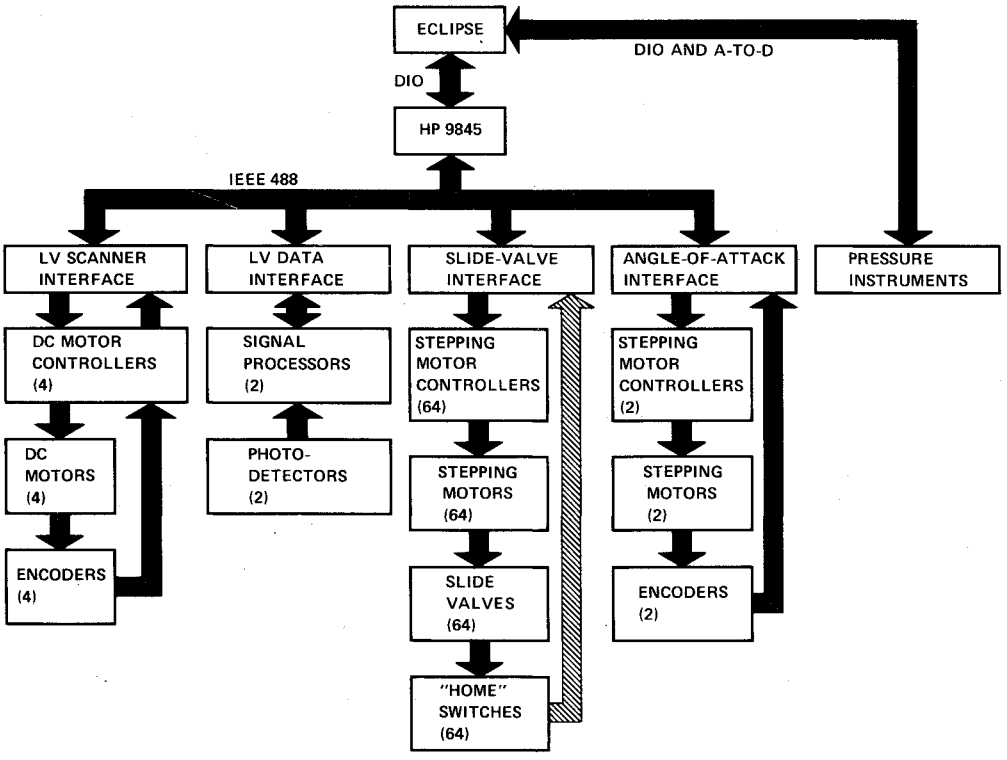

Fig. 5 Schematic of test-section data and control system.

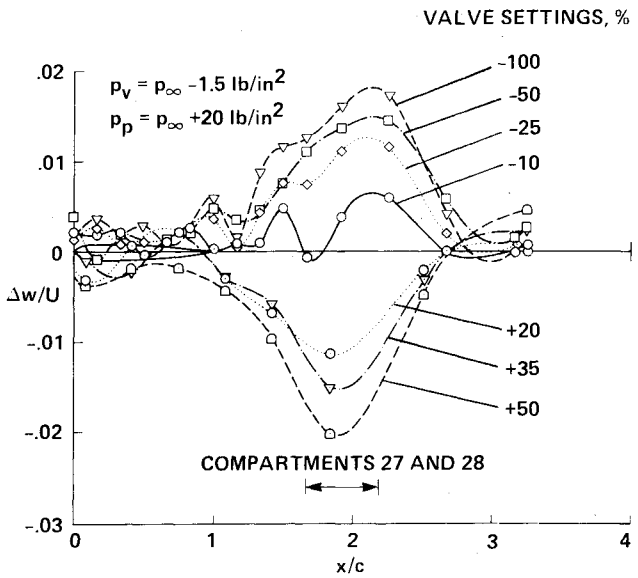

Fig. 6 Changes in vertical velocity at level $z/c = 1.5$ for various settings of valve pair 27-28.

The velocimeter was realigned between runs by a computer-controlled alignment system. The angles of the turning mirrors on the scanners were controlled by motorized micrometers, and the position of one of the laser beams at each mirror was measured by a position-sensitive photodetector mounted behind the mirror. The backs of the mirrors had been polished to allow the small fraction of light transmitted through the mirror to strike the detector.

Each velocity measurement was based on 100 samples. At Mach 0.80, the LV could resolve each sample to within 0.004 U in both axial and vertical directions. Most of the tests were run without artificial seeding since the presence of vaporized oil from the main-drive motors resulted in data rates of 50–70 samples per second.

Pressure Instrumentation

The model and plenum-pressure distributions were measured by pneumatic multiplexers with differential-pressure transducers. Tunnel total temperature and pressure were measured in the settling chamber upstream of the test section. Test-section static pressure was measured at an orifice in the sidewall just upstream of the test section. These pressures, and the transducer reference and calibration pressures, were measured by Paroscientific absolute-pressure transducers.

Computers and Control Systems

Two computers controlled the test section and the data acquisition system (Fig. 5). The host computer, a Data General Eclipse S/200, executed programs that included the logic for measuring and assessing wall interference and for adjusting the airflow through the walls. A Hewlett Packard HP-9845 desktop computer was interfaced to the test section hardware and received its instructions from the host computer across a 16-bit digital input/output (DIO) interface.

The slide valve, laser velocimeter, and angle-of-attack systems were each connected to the IEEE 488 interface bus of the HP-9845 through separate programmable interfaces. The pressure instrumentation was connected directly to the DIO and analog-to-digital interfaces of the Eclipse computer.

The slide-valve control system allowed any combination of the 64 valves to be moved simultaneously, with each valve moving a different distance if desired. The only feedback to the control system came from home switches near the end of travel of each valve. The laser velocimeter control system allowed all axes of the scanners to be moved simultaneously. Feedback to the control system was provided by optical encoders mounted at the motor shafts. The HP-9845 controlled data acquisition and the Eclipse reduced the raw data. The angle-of-attack control system was closed loop and consisted of identical channels of electronics connected to each end of the model.

A third computer, a General Electric Series Six, controlled the auxiliary pumps. It maintained the set points of the high- and low-pressure reservoirs at approximately $p_\infty + 20$ psi and $p_\infty - 2$ psi, respectively, while also maintaining the pumps

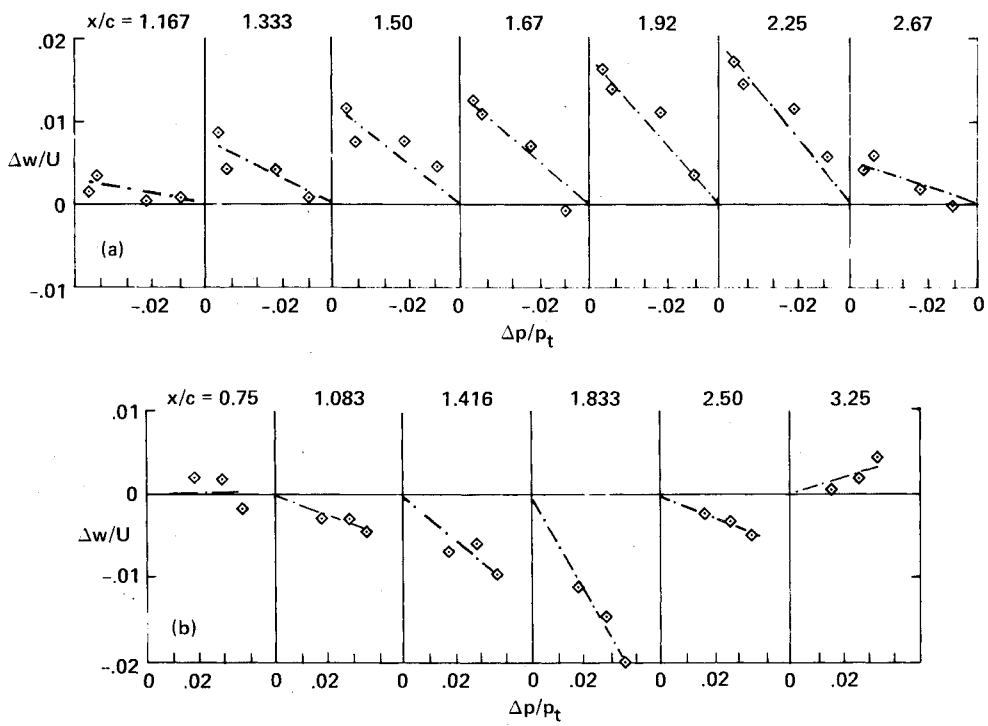

Fig. 7 Vertical velocity changes at level $z/x = 1.5$ vs pressure changes in plenum compartment 27.

within their safe operating limits. The response time of the control system was too long to prevent pressures in the reservoirs from exceeding their limits when all the slide valves moved simultaneously. However, slide valves could be adjusted individually and in pairs without restrictions.

The test-section Mach number was set manually by adjusting the tunnel main drive and monitoring the test-section total and static pressures.

Procedure

The procedure for adjusting the flow through the test-section walls involved three steps: 1) measuring flow conditions along a contour surrounding the model; 2) testing the measurements for compatibility with free-air boundary conditions (interference assessment); and 3) adjusting the plenum pressures to improve this compatibility (wall control). A fourth step, estimating wall-induced velocities near the model, was not essential, but was included as a way to quantify wall interference.

Velocity Measurements

The contour was a rectangle defined by two axial lines one and one-half chord lengths above and below the model (Fig. 2). These lines were as close to the walls as measurements could be made and, thus, were where the effects of plenum-pressure changes could most easily be measured. Axial and vertical velocities were measured at 16 points along each line. The points were centered with respect to adjacent pairs of plenum compartments. Data were interpolated at two lower points that were blocked from view by the angle-of-attack mechanism (Fig. 2).

Interference Assessment

For the nonlifting cases, the rectangular contour was assumed to extend beyond the ends of the test section to infinity. It divided the region outside the contour (outer flow) into upper and lower half-planes. Assuming free-air conditions at infinity and assuming that the outer flow obeys the linear Prandtl-Glauert equation, axial and vertical velocity distributions along the edge of a half-plane are related by relationships first published by Sears[1]:

$$u_m(x,z) = \frac{1}{\beta\pi}\int_{-\infty}^{\infty} \frac{w_m(\xi,z)}{x-\xi}\,d\xi \tag{1a}$$

$$w_m(x,z) = \frac{-\beta}{\pi}\int_{-\infty}^{\infty} \frac{u_m(\xi,z)}{x-\xi}\,d\xi \tag{1b}$$

These relationships were used to approximate the free-air distribution of each component from the measured distribution of the other. The approximations improved as wall interference was reduced. The integrals were evaluated numerically between the most upstream and downstream measurement points (Fig. 2), and velocities beyond the ends of the test section were assumed to be zero. For the highest-speed case ($M = 0.85$), free-air velocities were also computed by numerically estimating the solution to the transonic small perturbation equation in the region of the outer flow where perturbations were largest.[7]

For the lifting cases, the rectangular contour was assumed to be closed near the ends of the test section so as to avoid errors due to truncating the infinite integrals at these locations. Velocities along the upstream and downstream ends of the contour were interpolated from data at the endpoints of the measurement levels. The effect of the wake was ignored. In addition, the more restrictive assumptions of classical, linear, wall-interference theory were assumed to apply; i.e., the wind-tunnel flow was assumed to be the linear superposition of model- and wall-induced flows and the model was assumed to be small. These assumptions allow true free-air velocities to be computed from measured velocities in a single step[8,9]:

$$u_m(x,z) = \frac{u(x,z)}{2} + \frac{1}{2\beta\pi} \times \int_c \frac{[\beta^2(\eta-z)u(\xi,\eta) + (\xi-x)w(\xi,\eta)]\,d\xi - \beta^2[(\xi-x)u(\xi,\eta) - (\eta-z)w(\xi,\eta)]\,d\eta}{(\xi-x)^2 + \beta^2(\eta-z)^2} \tag{2a}$$

$$w_m(x,z) = \frac{w(x,z)}{2} - \frac{\beta}{2\pi} \times \int_c \frac{[(\xi-x)u(\xi,\eta) - (\eta-z)w(\xi,\eta)]\,d\xi + [\beta^2(\eta-z)u(\xi,\eta) + (x-\xi)w(\xi,\eta)]\,d\eta}{(\xi-x)^2 + \beta^2(\eta-z)^2} \tag{2b}$$

Here, the path of integration is the closed rectangular contour. Note that solutions above and below the model are coupled.

Wall Control

The objective of the wall-control phase of the algorithm was to adjust the slide valves in a way that would reduce differences between theoretical and measured upwash distributions at the measurement levels. We chose to control vertical rather than axial velocities because of our experience in previous tests and because of the intuitive relationship between plenum pressures and vertical velocities. As in the pilot tests, we assumed a linear relationship between changes in the vertical velocities at the measurement levels and pressure changes in the plenum compartments. The constants of proportionality, or influence coefficients were measured as part of the calibration of the test section. We also assumed that pressure changes in more than one plenum compartment had additive effects on vertical velocities and that pressure changes in the upper plenum had no effect on vertical velocities at the lower measurement level (and likewise for the effect of the lower plenum on the upper level). Exact solutions for the necessary plenum pressure changes were computed by multiplying the desired velocity changes by the inverse of the matrix of influence coefficients. Because the elements of exact solutions were, typically, very large numbers of alternating sign, approximate but more physically meaningful solutions were determined using the least-squares method of Lawson and Hanson.[10]

Applying the foregoing method presented several practical difficulties. For example, it was not possible to isolate the effects of pressure changes in a single plenum compartment because adjustments to a single slide valve changed the pressures in many compartments. Therefore, the influence coefficients were defined in terms of self-induced pressure changes, i.e., the pressure changes in each compartment produced by adjusting only the associated slide valve. By this definition, however, the wall controls had to be adjusted one at a time, making plenum pressure adjustments very time consuming. Therefore, to save time, adjacent slide valves were paired and driven in unison as if they were a single control. Velocity changes were correlated with the pressure change in the upstream compartment of each pair, and valve pairs were adjusted working downstream from the upstream end of the test section. As the valves were adjusted and tunnel blockage was reduced, the freestream Mach number generally increased. The desired Mach number was restored after the last pair of slide valves had been adjusted.

Results

Calibration

The principal task in the calibration of the present test section was measuring the wall-influence coefficients. Influence coefficients were measured at Mach 0.75 with the model installed at zero incidence. Valve pairs were adjusted one at a time with all other valves closed. Not all of the influence

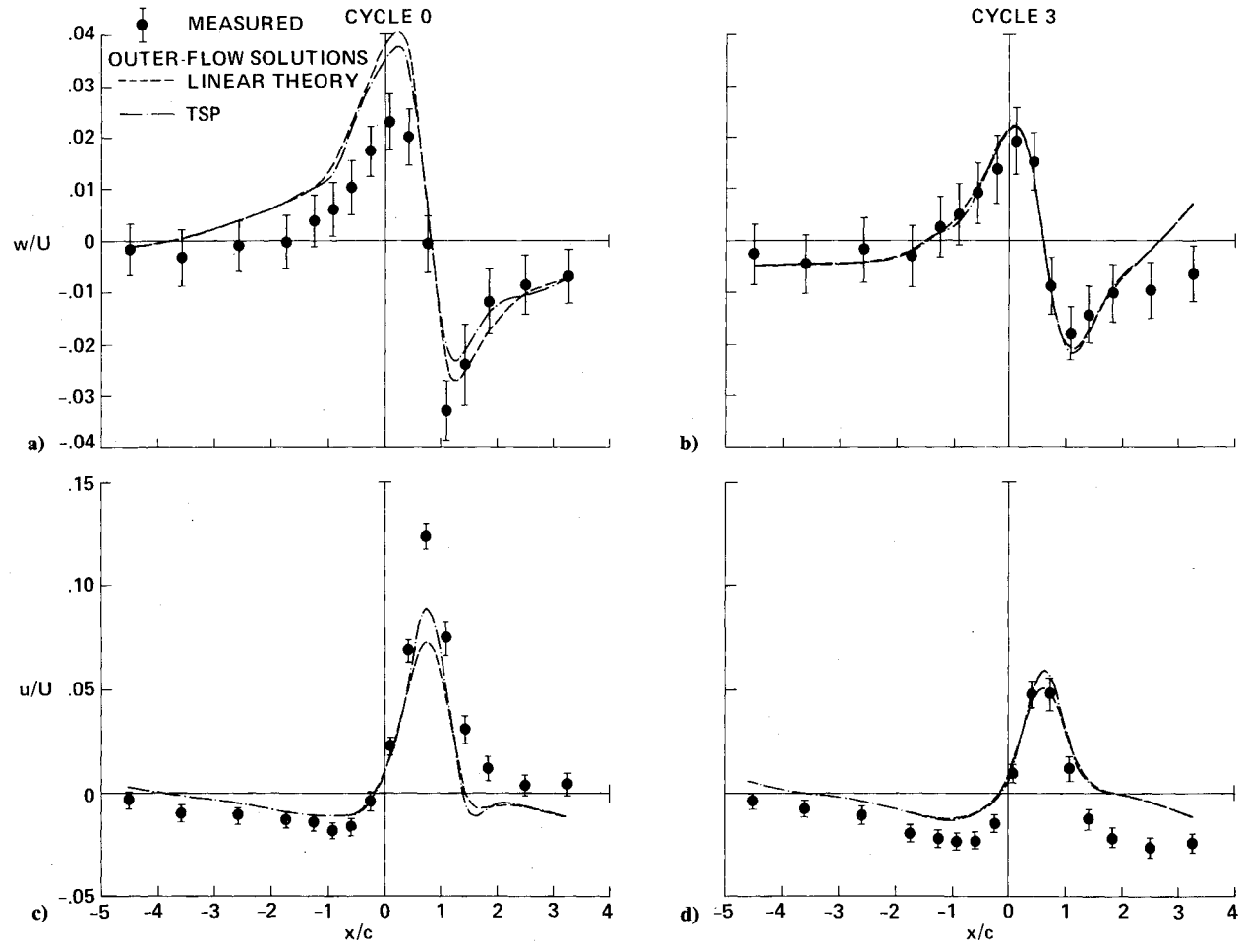

Fig. 8 Comparison of measured velocities at $z/c = 1.5$ with the outer-flow solutions before and after wall adjustments ($M = 0.85$, $\alpha = 0$ deg).

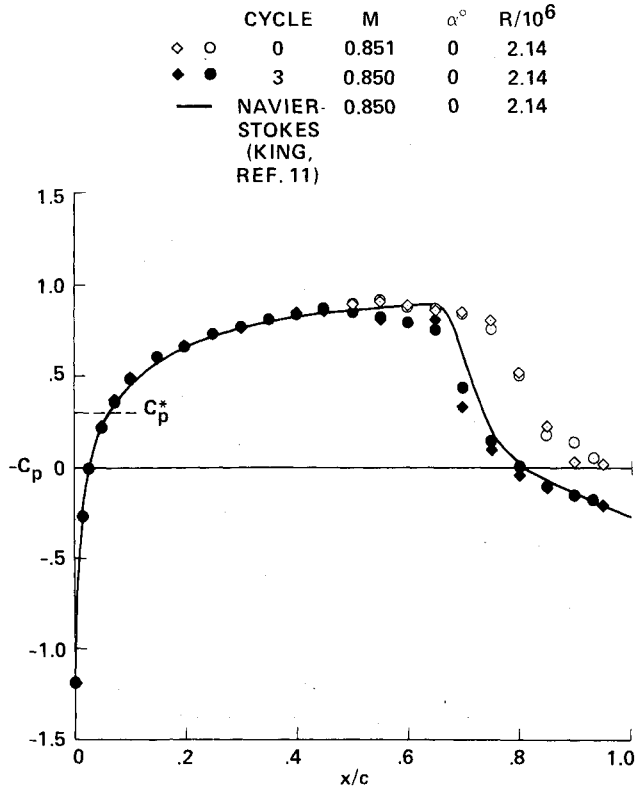

Fig. 9 The effect of wall adjustments on the model pressure distribution ($M = 0.85$, $\alpha = 0$ deg).

coefficients were measured; the data were generalized by assuming that the influence coefficients of all compartments of the same size were the same (after accounting for differences in the distances between the compartments and the measurement points). Figure 6 illustrates typical changes in vertical velocity for various settings of one pair of slide valves. As expected, suction (negative valve settings) produced an upwash, and blowing (positive valve settings) produced a downwash, immediately below the active compartments. Furthermore, the magnitudes of the disturbances increased with increased valve openings. Figure 7 is a cross plot of the same data and includes straight lines passing through the origin that give the best least-squares fit of the data. The slopes of these lines were defined as the influence coefficients.

Adaptive-Wall Experiments

The adaptive-wall algorithm was applied with the model at angles of attack of 0 and 2 deg and at freestream Mach numbers between 0.70 and 0.85. The Reynolds number for all of the tests was approximately 2×10^6 (corresponding to atmospheric stagnation conditions). Results for two cases, one nonlifting and the other lifting, are presented in the following.

Nonlifting Case ($M = 0.85$, $\alpha = 0$ Deg)

Since both the airfoil (NACA 0012) and the walls of the test section were symmetrical, we assumed for nonlifting cases that the flowfield was also symmetrical about the centerline of the test section ($z/c = 0$). Therefore, we measured flow conditions above the model only and applied the wall-control algorithm to the upper wall. To maintain flow symmetry, the lower slide valves were commanded to make exactly the same moves as the corresponding upper valves. Outer-flow solutions were computed using both linear and nonlinear theory, assuming an

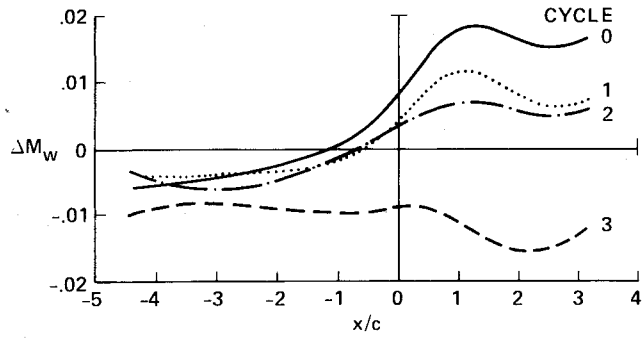

Fig. 10 The effect of wall adjustments on the wall-induced Mach number along the test-section centerline, $z/c = 0$ ($M = 0.85$, $\alpha = 0$ deg).

infinite contour, and without extrapolating the data beyond the ends of the test section.

The initial slide-valve settings for this case were the final settings for a nonlifting case run at $M = 0.835$. Most of the slide valves were about 10% open to the vacuum reservoir; valves immediately above and the below the model were further open to vacuum and no valves were open to the pressure reservoir. The adaptive-wall algorithm was applied three times, each time using only 25% of the correction indicated by the interference assessment (i.e., the relaxation factor was 0.25). By the end of the last cycle of plenum-pressure adjustments, all of the slide valves immediately above and below the model were fully open to the low-pressure reservoir.

Figures 8 show how the wall adjustments reduced differences between the measured and theoretical velocity distribu-

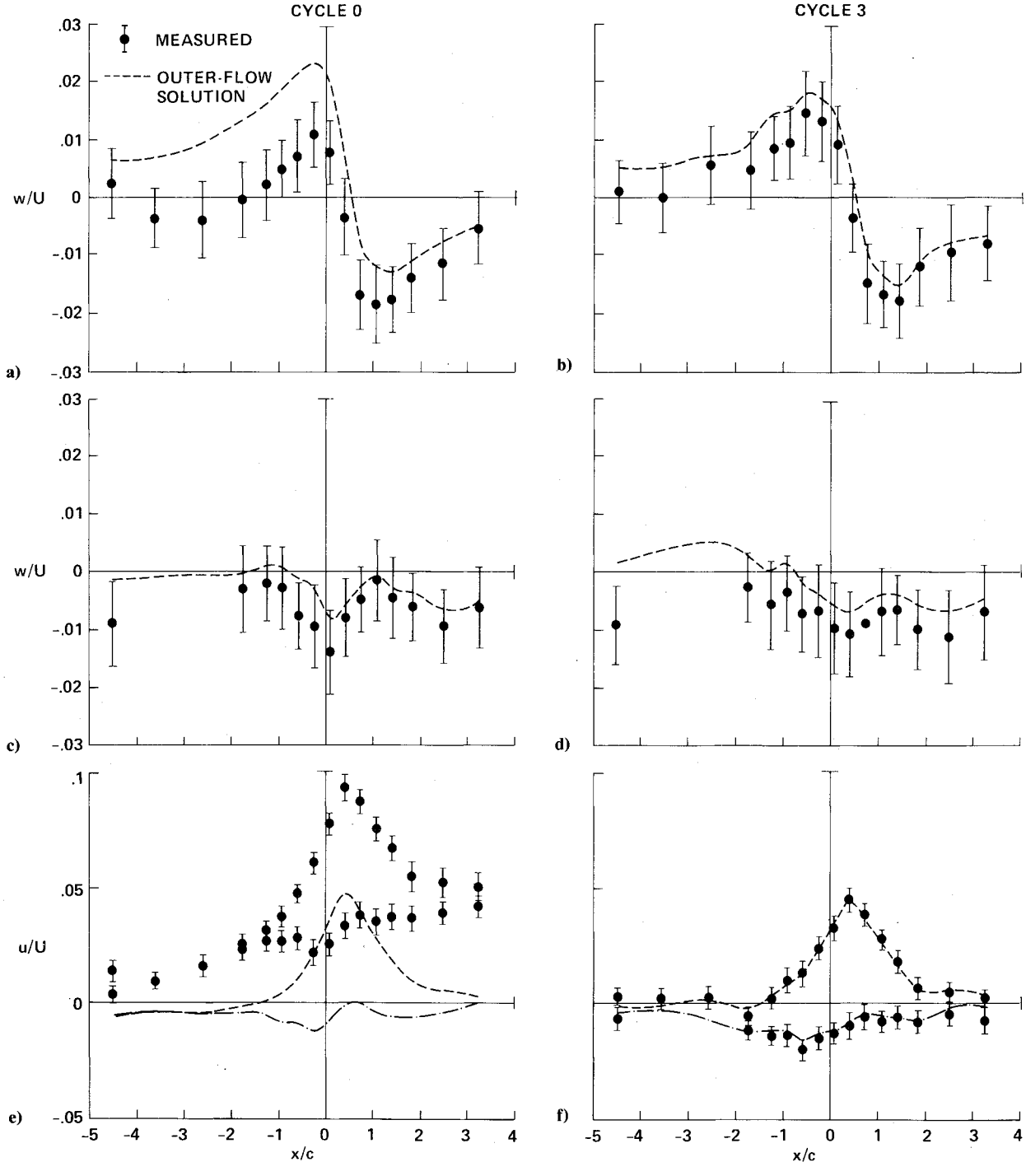

Fig. 11 Comparison of measured velocities with the outer-flow solutions before and after wall adjustments ($M = 0.70$, $\alpha = 2.0$ deg).

tions at the measurement level. Each LV data point includes an error bar of length equal to the rms of the measurement. Except at the two most downstream measurement points, the vertical velocity distribution was well corrected by the pressure adjustments (compare Figs. 8a and 8b). The plenum-pressure adjustments substantially reduced axial velocities and improved the agreement with the outer-flow solution immediately above the model (compare Figs. 8c and 8d). Axial velocities downstream of the model were significantly overcorrected. Differences between the linear and nonlinear outer-flow solutions were small because the supersonic bubble produced by the model did not extend to the measurement level.

The plenum-pressure adjustments moved the shock wave on the model upstream, as if the freestream Mach number had been reduced, and eliminated flow separation near the model's trailing edge (Fig. 9). This is consistent with the reduction of axial velocities at the measurement level, evident in Fig. 8d. Figure 9 compares the experimental pressure distributions with a numerical solution to the Reynolds-averaged, Navier-Stokes equations for the model in free air.[11] The plenum-pressure adjustments improved the agreement between experimental and theoretical data. The position of boundary-layer transition was fixed at $x/c = 0.05$ in the calculations and was unknown in the experiments.

Figure 10 illustrates wall-induced axial velocities along the centerline of the test section ($z/c = 0$) computed from the velocity measurements using a linear, two-component, closed-contour, wall-interference assessment and correction (WIAC) method.[7,9] Initially, the walls produced a positive Mach number increment near the model, as well as a large axial Mach number gradient. The plenum-pressure adjustments progressively reduced the wall-induced Mach number and its gradient, and the last cycle resulted in a substantial overcorrection. This result is consistent with the upstream movement of the shock wave. Wall-induced vertical velocity along the tunnel centerline was zero by the assumption of flow symmetry.

In a subsequent nonlifting case in which flow measurements were made below the model as well as above it, there was a 0.5-deg flow-angle offset between upper and lower vertical-velocity distributions. It is likely that there was a similar offset in the present case. Better results might have been achieved had the upper and lower slide valves been adjusted independently.

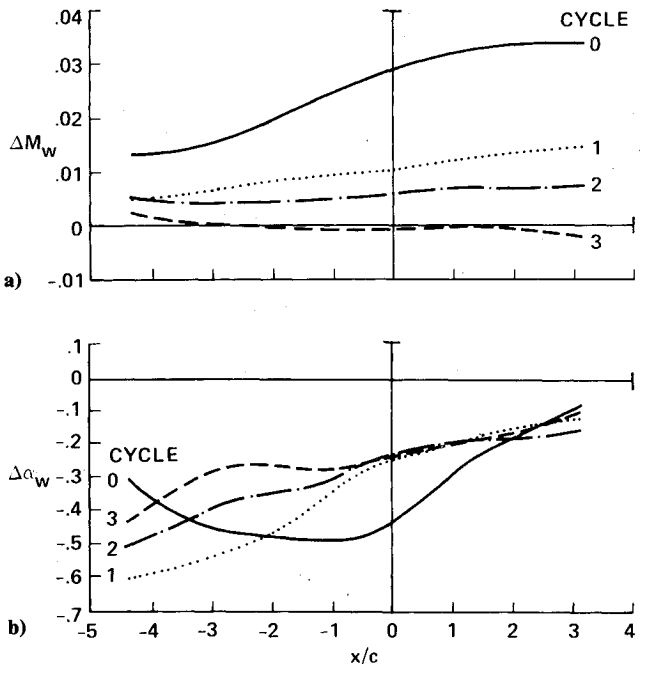

Fig. 12 The effect of wall adjustments on the wall-induced velocities along the test section centerline, $z/c = 0$ ($M = 0.70$, $\alpha = 2.0$ deg).

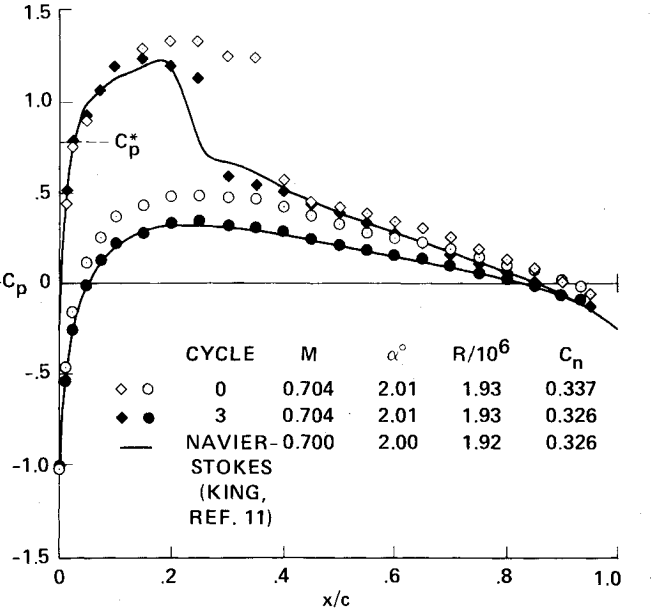

Fig. 13 The effect of wall adjustments on the model pressure distribution ($M = 0.70$, $\alpha = 2.0$ deg).

Lifting Case ($M = 0.70$, $\alpha = 2.0$ Deg)

All of the slide valves were initially closed. Flow measurements were made above and below the model, and outer-flow solutions were computed using the closed-contour, one-step method [Eqs. (2a) and (2b)]. The relaxation factor for all plenum-pressure adjustments was 1.0.

With all valves closed, there were large differences between measured and theoretical vertical velocities above the model, and smaller differences below the model (Figs. 11a and 11c). The measured axial velocities were substantially larger than the outer-flow solutions both above and below the model along the entire length of the test section (Fig. 11e).

Because the interference of the lower wall was expected to be small, only the upper plenum-pressures were adjusted. After three cycles of adjustments, measured and theoretical vertical-velocity distributions above the model were in substantially better agreement with each other (Fig. 11b). As might be expected, there was no corresponding improvement below the model (Fig. 11d). The pressure adjustments dramatically improved the agreement between computed and measured axial velocities both above and below the model (Fig. 11f).

Wall-induced axial velocities along the tunnel centerline were all but eliminated by the pressure adjustments (Fig. 12a), and, although the first cycle of adjustments reduced the wall-induced downwashes and their streamwise gradient, the subsequent two cycles had little further beneficial effect and left significant residual wall-induced downwash (Fig. 12b). This is consistent with the offset between the measured and outer-flow upwash distributions in Figs. 11b and 11d. The plenum-pressure adjustments shifted the shock wave on the model slightly upstream and reduced the suction on the airfoil's lower surface (Fig. 13). The normal force coefficient decreased slightly.

Discussion

The cases presented here were typical of all of the cases that were investigated. Wall interference was always significantly reduced but never to levels low enough to make corrections for residual interference unnecessary. The principal reason we could not reduce interference further was our inability to predict accurately the effects of plenum-pressure changes on velocity distributions. In particular, the influence coefficients were not known with sufficient accuracy (evident by the scatter in the data in Figs. 6 and 7) and they were based on

oversimplified assumptions (e.g., that they could be generalized from only a few measurements at a single Mach number and that the effect of pressure changes in many compartments could be determined by linear superposition). In addition, the quantity we chose to control, upwash, was far less sensitive to wall adjustments than axial velocity. A better approach might have been to determine the necessary plenum-pressure changes directly in terms of axial velocities, at least for cases dominated by blockage interference.

Further development of the test section is required before it would be suitable for production testing. In addition to the wall-control problems discussed here, the time required to adjust the slide valves (about 9 min/cycle) far exceeded the time that would be acceptable for production tests. The slide valves could be adjusted in a matter of seconds instead of minutes if an accurate method were available that allowed them to be adjusted simultaneously rather than in pairs. LV data-acquisition times also need to be substantially reduced. Times approaching 1 min would be possible with proper seeding.

Concluding Remarks

First tests were conducted in an adaptive-wall test section in the NASA Ames 2- × 2-ft transonic wind tunnel. An automatic procedure was demonstrated that consistently reduced wall interference in transonic flow past a two-dimensional airfoil. This conclusion is based on 1) comparisons of measured axial and vertical velocity distributions with outer-flow solutions; 2) calculations of wall-induced velocities near the model; and 3) comparisons of the model pressure distribution with computational fluid dynamics solutions for the model in free air.

Measurable and significant interference remained after the last plenum-pressure adjustments. The foremost reason for this was that the influence matrix did not represent accurately the relationships between pressure changes in the plenum compartments and vertical-velocity changes at the measurement levels.

Further development of the adaptive-wall test section is required before it will be suitable for production testing. Specifically, the method for determining the proper wall adjustments must be improved, and the time required to execute the algorithm must be drastically reduced. Shorter execution times could be achieved by improving the seeding of the laser velocimeter and by developing a wall-control method that allows all the slide valves to be adjusted simultaneously.

References

[1]Sears, W. R., "Self-Correcting Wind Tunnels," *Aeronautical Journal*, Vol. 78, Feb.–March 1974, pp. 80–89.

[2]Wolf, S. W. D., "Evaluation of a Flexible Wall Testing Technique to Minimize Wall Interferences in the NASA Langley 0.3-Meter Transonic Cryogenic Tunnel," AIAA Paper 88-0140, Jan. 1988.

[3]Chevallier, J. P., Mignosi, A., Archambaud, J. P., and Seraudie, A., "T2 Wind Tunnel Adaptive-Walls: Design, Construction and Some Typical Results," *La Recherche Aérospatiale* (English edition), No. 4, 1983, pp. 1–19.

[4]Lewis, M. C., "Aerofoil Testing in a Self-Streamlining Flexible Walled Wind Tunnel," NASA CR-4128, May 1988.

[5]Satyanarayana, B., Schairer, E. T., and Davis, S. S., "Adaptive-Wall Wind Tunnel Development for Transonic Testing," *Journal of Aircraft,* Vol. 18, No. 4, 1981, pp. 273–279.

[6]Davis, S. S., "A Compatibility Assessment Method for Adaptive-Wall Wind Tunnels," *AIAA Journal*, Vol. 19, No. 9, 1981, pp. 1169–1173.

[7]Schairer, E. T., "Methods for Assessing Wall Interference in the Two- by Two-Foot Adaptive-Wall Wind Tunnel," NASA TM-88252, June 1986.

[8]Everhart, J. L., "A Method for Modifying Two-Dimensional Adaptive Wind-Tunnel Walls Including Analytical and Experimental Verification," NASA TP-2081, Feb. 1983.

[9]Mokry, M., Chan, Y. T., and Jones, D. J., "Two-Dimensional Wind Tunnel Wall Interference," AGARDograph 281, Nov. 1983.

[10]Lawson, C. L., and Hanson, R. J., *Solving Least-Squares Problems*, Prentice Hall, Englewood Cliffs, NJ, 1974.

[11]King, L. S., "A Comparison of Turbulence Closure Models for Transonic Flows about Airfoils," AIAA Paper 87-0418, Jan. 1987.